Available online at www.sciencedirect.com
ScienceDirect
Thin Solid Films 515 (2006) 333 – 337
www.elsevier.com/locate/tsf

Influence of the nature of oxide matrix on the photoluminescence spectrum of ion-synthesized silicon nanostructures

D.I. Tetelbaum [a,b,*], O.N. Gorshkov [a], A.V. Ershov [a], A.P. Kasatkin [a], V.A. Kamin [a], A.N. Mikhaylov [a,b], A.I. Belov [a], D.M. Gaponova [c], L. Pavesi [d], L. Ferraioli [d], T.G. Finstad [e], S. Foss [e]

[a] University of Nizhny Novgorod, 23/3 Gagarin ave., Nizhny Novgorod, 603950, Russia
[b] Surface Phenomena Research Group, 9/23 2-nd Baumanskaya str., Moscow, 105005, Russia
[c] Institute for Physics of Microstructures RAS, GSP-105, Nizhny Novgorod, 603950, Russia
[d] Dipartimento di Fisica, University of Trento, via Sommarive 14, Povo (Trento), 38050, Italy
[e] University of Oslo, PO Box 1048, Blindern, 0316 Norway

Available online 31 January 2006

Abstract

The photoluminescence of various Si ion implanted oxide layers annealed at high-temperature has been studied in the range of 350–1500 nm. The set of investigated oxide materials includes thermal SiO_2, deposited SiO_2, $Si_{0.9}Ge_{0.1}O_2$, GeO_2 films on silicon substrate, and sapphire wafers. The results are discussed in terms of generation and modification of the defect centers and nanoclusters formation taking into account several factors related to composition and structure of the original oxide matrices.
© 2005 Elsevier B.V. All rights reserved.

Keywords: Nanostructures; Oxides; Ion implantation; Photoluminescence

1. Introduction

Ion-beam nanostructuring of oxides is widely studied due to their prospective as nano- and optoelectronic materials. Most of the works are devoted to SiO_2, for which the processes of Si nanocrystals ion-beam synthesis and corresponding luminescence have been investigated in details [1,2]. The effects of Si implantation into other oxides have been investigated to a lesser extent. The combination of the specific properties of some oxides with the unique properties of Si nanocrystals would greatly expand the range of their applications. For instance, Al_2O_3 is considered as one of the potential high-k replacements for SiO_2 in CMOS-technology [3]. While $Si_{1-x}Ge_xO_2$ ($x<1$) and GeO_2 oxides are photosensitive and change their refractive index under UV irradiation enabling fabrication of planar optical waveguides/gratings [4]. They also act as active media in effective Raman amplifiers [5]. Therefore, synthesis of luminescent Si nanocrystals in these oxide matrices could produce novel multifunctional materials. However, no systematic approach to study the formation of light-emitting centers (defects or nanocrystals) in these different oxides has been performed up to now. In the present letter, we compare photoluminescence (PL) properties of the nanostructures obtained by Si ion implantation into SiO_2, $Si_{0.9}Ge_{0.1}O_2$, GeO_2, and Al_2O_3 layers followed by high temperature annealing.

2. Experimental details

SiO_2 films (500 nm) grown by wet oxidation, SiO_2 (120 nm) deposited on silicon substrate by electron beam evaporation, $Si_{0.9}Ge_{0.1}O_2$ (250 nm) and GeO_2 (300 nm) films deposited on silicon or fused quartz substrates by rf-magnetron sputtering, and R-plane sapphire wafers were used as the initial materials. Si^+ (and Ar^+) ion implantation was performed with 100 keV energy and doses ranging from $3\cdot10^{16}$ to $3\cdot10^{17}$ ions/cm^2. The samples were subsequently annealed at 500–1100 °C under dry

* Corresponding author. University of Nizhny Novgorod, 23/3 Gagarin ave., Nizhny Novgorod, 603950, Russia. Tel.: +7 8312 656914; fax: +7 8312 659366.
E-mail address: tetelbaum@phys.unn.ru (D.I. Tetelbaum).

0040-6090/$ - see front matter © 2005 Elsevier B.V. All rights reserved.
doi:10.1016/j.tsf.2005.12.088

nitrogen ambient for 2 h. Room-temperature PL in the range of 350–900 nm was excited by a 337 line of pulse N_2-laser (mean power of ~1 mW, repetition rate of 25 Hz) and detected by a photomultiplier tube. PL in the 600–1000 and 900–1500 nm ranges was excited by an Ar^+-laser (488 nm, ~850 mW) and detected by a CCD array or an InGaAs detector, respectively. The PL decay time measurements were performed on the implanted sapphire samples using excitation with 488 nm light of an optical parametric oscillator pumped by a Nd:YAG laser with pulse duration of 6 ns, repetition rate of 10 Hz, and mean power of 2.9 mW. The cross-sectional transmission electron microscopy (TEM) micrographs and diffraction patterns were obtained by using JEOL 2010F transmission electron microscope and 200 keV electrons focused on areas about 100 nm thick.

3. Results and discussion

Fig. 1 shows the influence of Si^+ implantation and annealing on the PL spectra of thermal (a) and deposited (b) SiO_2 films. As can be seen, the spectra of the initial oxides are

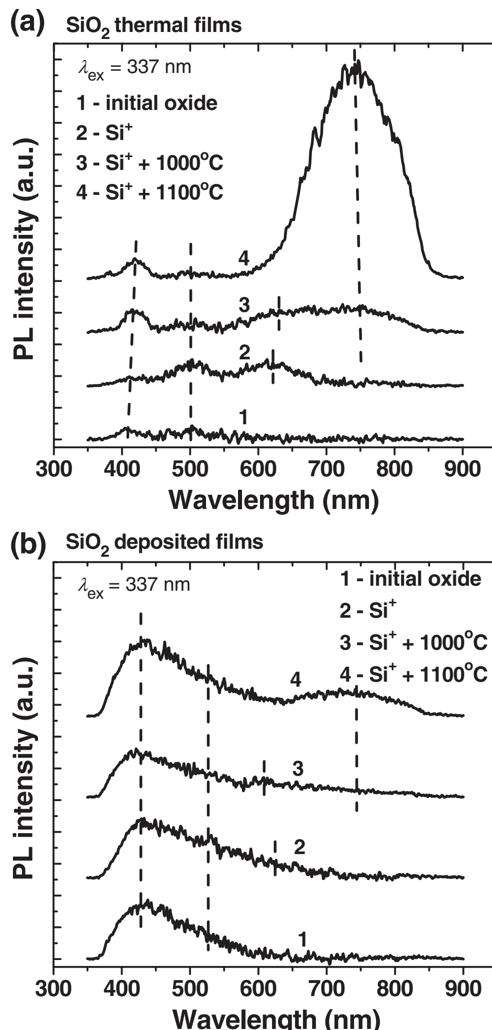

Fig. 1. Influence of Si^+ ($1\cdot10^{17}$ ions/cm^2) ion implantation and subsequent annealing on the visible PL spectra of thermal (a) and deposited (b) SiO_2 films.

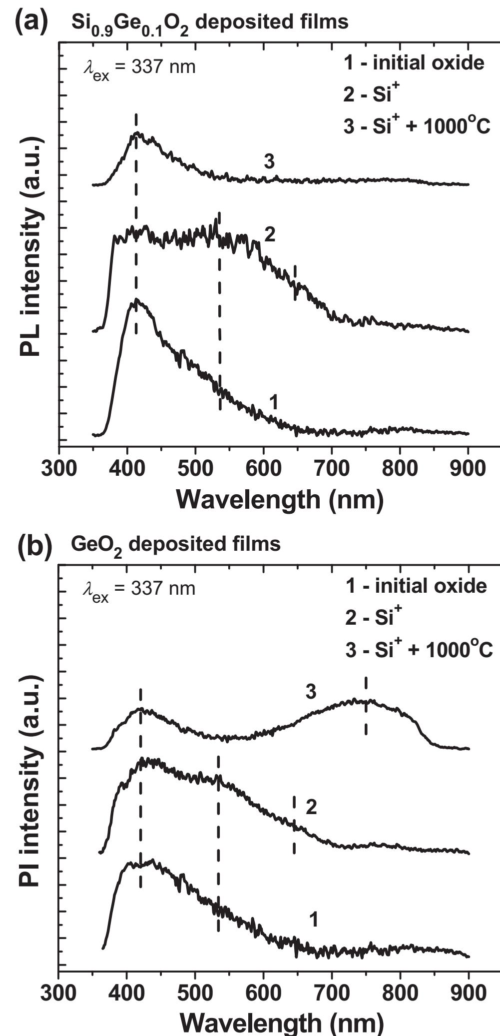

Fig. 2. Influence of Si^+ ($1\cdot10^{17}$ ions/cm^2) ion implantation and subsequent annealing on the visible PL spectra of deposited $Si_{0.9}Ge_{0.1}O_2$ (a) and GeO_2 (b) films.

characterized by the presence of defect-related emission in the range of 350–600 nm. In case of thermal SiO_2 film two PL peaks at 405 and 500 nm are well resolved, but, for the deposited silicon oxide, we observe a broad PL band. The broadening is caused by a larger deviation from stoichiometry and a variety of defect modifications in the latter case. According to the numerous literature sources (for example see [6–8]), these PL peaks can be attributed to the twofold coordinated Si atom and neutral oxygen vacancy, respectively. The Si^+ ion implantation modifies PL spectrum resulting in the decrease of 400–450 nm PL, the increase of 500–550 nm PL and the appearance of a PL peak (Fig. 1a) or of a weak shoulder (Fig. 1b) at 600–700 nm. This behavior is more evident in case of thermal oxide and can be explained by the fact that ion irradiation introduces nonradiative *E'*-centers quenching PL [9] and radiative nonbridging oxygen hole centers responsible for the observed emission at 650 nm [10].

Annealing at 1000–1100 °C of the Si-implanted SiO_2 films leads to the appearance of a PL peak centered at 750 nm which unambiguously is not caused by the radiation-induced modification of the oxide defect structure [9]. The strong correlation

between the data of scrupulous high-resolution electron microscopy study and size-dependent evolution of the PL [1,11] allows to associate this 750 nm emission with radiative transitions in Si nanocrystals with size of 3–5 nm. The nanocrystal-related emission is more intense for 1100 °C annealing because of the temperature dependence of Si nanocrystals nucleation rate [12]. For 1000 °C, this PL peak is accompanied by a shoulder at 600–650 nm typical of emission from non-crystalline Si clusters considered as nanocrystal precursors [13,14]. It is also seen that the nanocrystal formation is less effective in the relatively defective deposited SiO_2 film probably due to the trapping of Si excess atoms into extended defects such as voids and/or density fluctuations which slow down the Si diffusion.

The typical PL spectra of rf-deposited $Si_{0.9}Ge_{0.1}O_2$ and GeO_2 films are shown in Fig. 2. These oxides show similar defect related emissions. The main difference is that a wide emission band at 750 nm appears only in the Si^+-implanted and then annealed GeO_2 films. This band non-monotonously depends on the Si dose [15] and can be attributed to Si nanocrystals formation. Since we have no direct evidence for the synthesis of Si nanocrystals during decomposition of GeO_2:Si solid solution in our case, the interpretation suggested here seems hypothetical. However, to the best of our knowledge, no defect luminescence in the range of 700–900 is observed in the annealed silicon–germanium oxides except for hydrogen-loaded ones [16]. The difference between $Si_{0.9}Ge_{0.1}O_2$ and GeO_2 can result from local stresses introduced by Ge atoms in the *mixed* oxide. Stress could make energetically more favorable for introduced Si atoms to substitute Ge than to clusterize as Si nanocrystals. This is supported by the observation of a PL shoulder at 935 nm on the Si substrate emission in the spectrum of Si^+-implanted and annealed $Si_{0.9}Ge_{0.1}O_2$ film (Fig. 3). This PL feature can be related to Ge (or SiGe alloy) nanocrystals composed of replaced Ge atoms. Such nanocrystals were shown to form during annealing of the mixed layers deposited by co-sputtering of Si, Ge, and SiO_2 targets, as well as to emit light

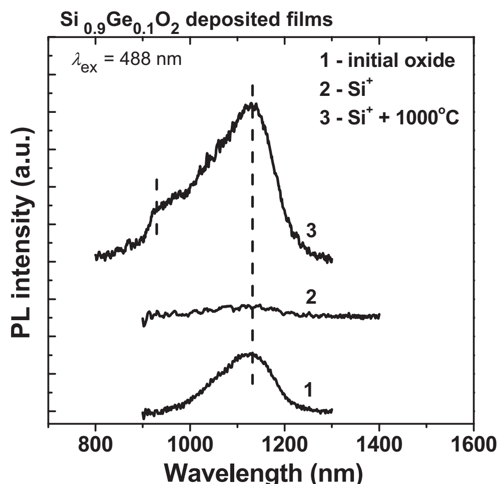

Fig. 3. Influence of Si^+ ($1 \cdot 10^{17}$ ions/cm^2) ion implantation and subsequent annealing on the near-infrared PL spectra of deposited $Si_{0.9}Ge_{0.1}O_2$ films.

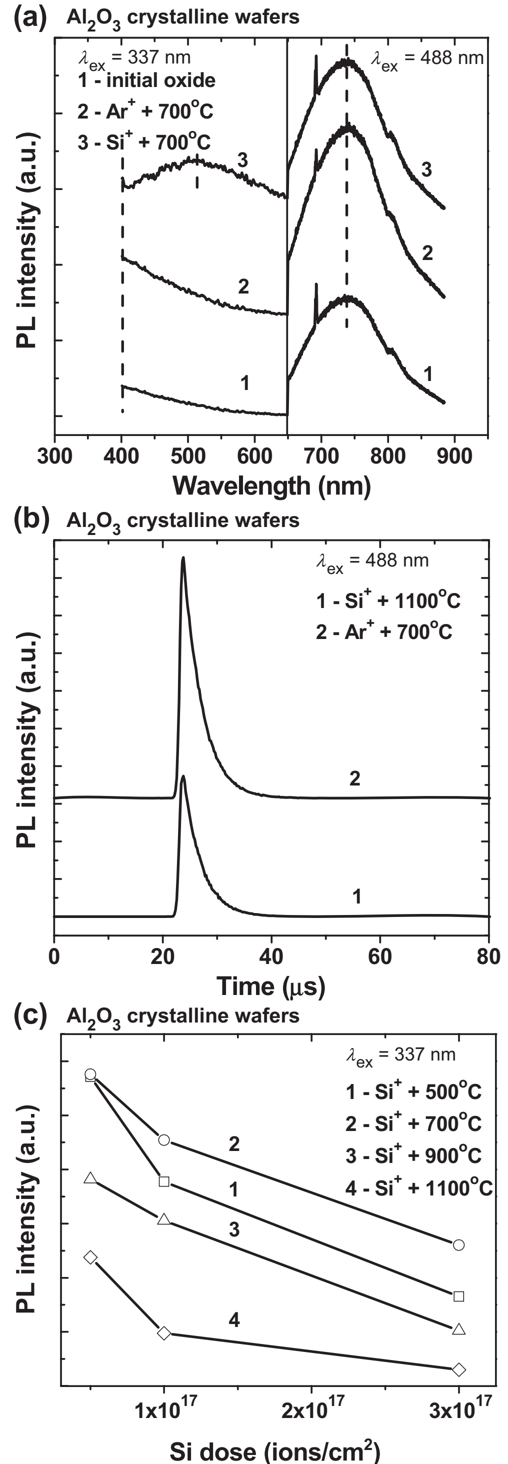

Fig. 4. Influence of Si^+ ($1 \cdot 10^{17}$ ions/cm^2), Ar^+ ($8 \cdot 10^{16}$ ions/cm^2) ion implantation and subsequent annealing on the PL spectra of sapphire (a); 740 nm PL decay curves of the sapphire samples implanted by the same doses of Si^+ and Ar^+ ions and subsequently annealed (b); the dependence of the 500 nm PL intensity on the Si^+ dose for various annealing temperatures (c).

in the near-infrared range of spectra due to quantum confinement effect [17].

The initial sapphire samples (Fig. 4a) display a luminescence at around 400 nm and originated from the well known *F*-centers (oxygen vacancies trapping two electrons) [18].

Another PL peak at 740 nm is excited by the 488 nm laser. Although the position of this peak coincides with emission from Si nanocrystals in SiO_2, such an interpretation is problematic because this PL is observed for the original and Ar^+-implanted sapphire as well. Moreover, this PL peak is very similar to that of Ti^{3+}-doped Al_2O_3 [19]. PL decay times of the 740 nm emission, reported in Fig. 4b, show lifetimes of 3.4 and 3.5 μs for Si^+ and Ar^+-implanted sapphire samples. The data were obtained with integration on a 90 nm wide wavelength range, centered at 740 nm. These lifetimes are in good agreement with values reported for Ti^{3+} radiative transition in Al_2O_3 [19]. The sharp PL peaks observed at 690 nm (Fig. 4a) are evidently caused by the Cr^{3+}-centers [20] also present in our sapphire samples.

A PL band with maximum at 500 nm appears only after annealing of Si-implanted Al_2O_3 (Fig. 4a). A similar cathodoluminescence peak at 570 nm has been recently reported for sapphire layers containing Si nanocrystals [21]. It is reasonable to relate this emission to Si nanocrystals. Intensity of the observed "orange" PL reaches its maximal value after annealing at 700 °C and monotonically falls down with rising the Si dose in the investigated range (Fig. 4c). Assuming quantum size effect as the origin, this behavior can be explained by the corresponding increase of Si nanocrystal size.

The preliminary results of TEM and electron diffraction analysis give direct evidence for the synthesis of Si nanocrystals in our Si^+-implanted sapphire samples. A cross-sectional TEM micrograph of the sample implanted with the highest Si dose ($3 \cdot 10^{17}$ ions/cm^2) after annealing at 900 °C is shown in Fig. 5a. The surface Al_2O_3 layer is amorphous, and the annealing regime is not sufficient for its recrystallization. Nevertheless, the implanted Si has precipitated out in this layer as randomly oriented nanocrystals, clearly seen from the diffraction pattern displayed in Fig. 5b. After annealing at 1100 °C the Al_2O_3 has recrystallized, but contains many extended defects (Fig. 5c). Si nanocrystals are located at about 50–80 nm from surface, tend to be faceted and have a definite relationship to the orientation of the Al_2O_3 lattice as seen from the diffraction spots in Fig. 5d. The average Si nanocrystal size is roughly 10 nm.

The position of the 500 nm band is drastically blue-shifted from that of Si nanocrystals in SiO_2. The reason for this is unclear yet. We can speculate that we observe emission from very small Si nanocrystals or "non-phase" [13,14] (chain or ring-like) Si clusters. Another possibility is that mechanical stresses at the interfaces between nanocrystals and the crystalline matrix modify essentially the energy band structure of Si quantum dots resulting in the corresponding shift of the PL peak. One more possibility consists in the direct radiative transition in the Si nanocrystal core without both the charge trapping into radiative interface states and the contribution of the interface local vibrations, which provide large Stokes shift

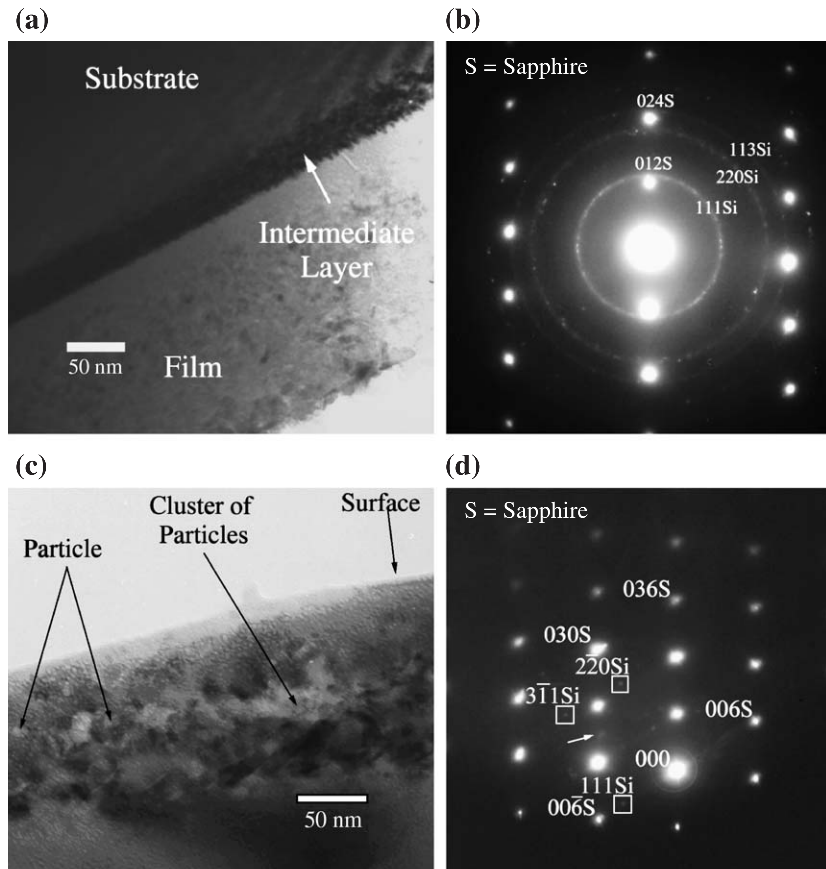

Fig. 5. TEM micrographs (a, c) and the corresponding electron diffraction patterns (b, d) of the sapphire samples implanted with Si^+ ($3 \cdot 10^{17}$ ions/cm^2) and annealed at 900 °C (a, b) and 1100 °C (c, d).

of the luminescence in case of SiO_2 matrix [1]. The exact origin of the "orange" PL band will be a subject of further investigations.

4. Conclusions

In summary, we have studied both the common and specific features of the PL from Si^+-implanted and annealed oxides. It has been shown that the formation and the properties of radiative defects and Si nanocrystals depend strongly on the composition and nature of the oxide matrix. To have a comprehensive model more work is needed.

Acknowledgments

Support of RFBR, Russian Ministry for Education and Science, CRDF (Award Nos. RUR1-1038-NN-03 and Y2-P-01-09), and EC project SEMINANO is gratefully acknowledged.

References

[1] B. Garrido Fernandez, M. Lopez, C. Garcia, A. Perez-Rodriguez, J.R. Morante, C. Bonafos, M. Carrada, J. Appl. Phys. 91 (2002) 798.
[2] P. Pellegrino, B. Garrido, C. Garcia, J. Arbiol, J.R. Morante, M. Melchiorri, N. Daldosso, L. Pavesi, E. Scheid, G. Sarrabayrouse, J. Appl. Phys. 97 (2005) 074312.
[3] G.D. Wilk, R.M. Wallace, J.M. Anthony, J. Appl. Phys. 89 (2001) 5243.
[4] K.O. Hill, Y. Fujii, D.C. Johnson, B.S. Kawasaki, Appl. Phys. Lett. 32 (1978) 647.
[5] E.M. Dianov, A.A. Abramov, M.M. Bubnov, A.M. Prokhorov, A.V. Shipulin, G.G. Devjatykh, A.N. Guryanov, V.F. Khopin, Electron. Lett. 31 (1995) 1057.
[6] V.B. Sulimov, V.O. Sokolov, J. Non-Cryst. Solids 191 (1995) 260.
[7] H. Nishikawa, T. Shiroyama, R. Nakamura, Y. Ohki, K. Nagasawa, Y. Hama, Phys. Rev., B 45 (1992) 586.
[8] F. Meinardi, A. Paleari, Phys. Rev., B 58 (1998) 3511.
[9] M.Ya. Valakh, V.A. Yukhimchuk, V.Ya. Bratus', A.A. Konchits, P.L.F. Hemment, T. Komoda, J. Appl. Phys. 85 (1999) 168.
[10] K. Kajihara, L. Skuja, M. Hirano, H. Hosono, Appl. Phys. Lett. 79 (2001) 1757.
[11] G.A. Kachurin, V.A. Volodin, D.I. Tetel'baum, D.V. Marin, A.F. Leer, A.K. Gutakovski, A.G. Cherkov, A.N. Mikhaylov, Semiconductors 39 (2005) 552.
[12] A.N. Mikhaylov, D.I. Tetelbaum, O.N. Gorshkov, A.P. Kasatkin, A.I. Belov, S.V. Morozov, Vacuum 78 (2005) 519.
[13] G.A. Kachurin, A.F. Leier, K.S. Zhuravlev, I.E. Tyschenko, A.K. Gutakovski, V.A. Volodin, W. Skorupa, R.A. Yankov, Semiconductors 32 (1998) 1222.
[14] L.X. Yi, J. Heitmann, R. Scholz, M. Zacharias, Appl. Phys. Lett. 81 (2002) 661.
[15] O.N. Gorshkov, Yu.A. Dudin, V.A. Kamin, A.P. Kasatkin, A.N. Mikhaylov, V.A. Novikov, D.I. Tetelbaum, Tech. Phys. Lett. 31 (2005) 509.
[16] K.D. Simmons, B.G. Potter Jr., G.I. Stegeman, Appl. Phys. Lett. 64 (1994) 2537.
[17] S. Takeoka, K. Toshikiyo, M. Fujii, S. Hayashi, K. Yamamoto, Phys. Rev., B 61 (2000) 15988.
[18] B.D. Evans, G.J. Pogatshnik, Y. Chen, Nucl. Instrum. Methods B 91 (1994) 258.
[19] L.E. Bausa, I. Vergara, F. Jaque, J. Garcia Sole, J. Phys., Condens. Matter 2 (1990) 9919.
[20] C. Jardin, B. Canut, S.M.M. Ramos, J. Phys., D, Appl. Phys. 29 (1996) 2066.
[21] C.J. Park, Y.H. Kwon, Y.H. Lee, T.W. Kang, H.Y. Cho, S. Kim, S.-H. Choi, R.G. Elliman, Appl. Phys. Lett. 84 (2004) 2667.